Calibration and performance characterization of a Mach 5 Ludwieg tube

View Online   Export Citation   CrossMark

Kyle P. Bearden,[a] Victor E. Padilla, Lutz Taubert, and Stuart A. Craig[b] (iD)

AFFILIATIONS

Department of Aerospace and Mechanical Engineering, University of Arizona, Tucson, Arizona 85721, USA

[a]**Present address:** Sandia National Laboratories, Albuquerque, New Mexico 87185, USA.
[b]**Author to whom correspondence should be addressed:** sacraig@arizona.edu

ABSTRACT

Calibration, commissioning, and design features of a new Mach 5 Ludwieg Tube wind tunnel at the University of Arizona are discussed. Mach number uniformity and free-stream noise levels are measured using a Pitot rake at a range of unit Reynolds numbers and at multiple spanwise and streamwise positions. The wind tunnel is shown to have a free-stream Mach number of 4.82 with maximum variance less than 0.8% (and less than 0.5% at most streamwise positions). The average free-stream acoustic noise level in the core (based on Pitot pressure) is shown to be less than 1.2% at an intermediate Reynolds number with some regions dropping locally below 1.0%. The core flow region is measured to be 282.4 mm (11.1 in.) in diameter at the nozzle exit.

Published under an exclusive license by AIP Publishing. https://doi.org/10.1063/5.0093052

I. INTRODUCTION

The University of Arizona (UArizona) has recently completed a four-year design, construction, and commissioning process for its new Mach 5 Ludwieg Tube (LT5). Ludwieg tubes provide a low-cost method for producing high-quality, high-speed flow for a short duration. In their simplest form, they are pressure–vacuum blowdown facilities where upstream tanks, regulators, and the settling chamber are replaced by a long driver tube.[1,2] The pressure and vacuum sides are separated, typically by diaphragms or a fast-opening valve, and flow is initiated by removing that barrier. As the resulting expansion wave propagates upstream through the nozzle, a quasi-steady flow is developed in the test section that lasts until the expansion wave reflects off of the upstream wall of the driver tube and returns to the nozzle.

The replacement of all upstream obstructions with an empty driver tube causes Ludwieg tubes to have a naturally low-disturbance flow approaching the nozzle throat. This feature has led them to become the design of choice in recent years when developing quiet hypersonic wind tunnels. Quiet tunnels were pioneered by NASA Langley Research Center in the second half of the 20th century[3,4] and are important tools in the study of boundary layer stability and transition due to their ability to produce a free-stream flow with very low noise intended to approximate that of flight. The development

and operation of quiet Ludwieg tubes was pioneered by Purdue University in the 1990s and 2000s with the development of Mach 4[5] and Mach 6[6] facilities, both of which are still in active use at the UArizona and Purdue, respectively.

LT5 has a cross section that is 381 mm (15 in.) in diameter and can operate at a range of pressures that make it a useful tool for both basic and applied research. The nozzle, at 3.5 m (11.5 ft) in length, is longer than a typical conventional nozzle and was designed to be sized similarly to a quiet nozzle of the same diameter and Mach number in order to facilitate a planned quiet nozzle upgrade. The tunnel shares vacuum and pressure infrastructure with the Mach 4 Quiet Ludwieg Tube (QLT4), which was recently acquired from Purdue and refurbished.[7]

This publication provides general operating parameters and describes the results of the flow quality assessment and free-stream characterization process performed during the commissioning of LT5.

II. EXPERIMENTAL APPARATUS
A. Wind tunnel facility

LT5, shown schematically in Fig. 1, is a typical Ludwieg tube design[1,2] with a driver tube that is 25.4 m (83.3 ft) in length and has
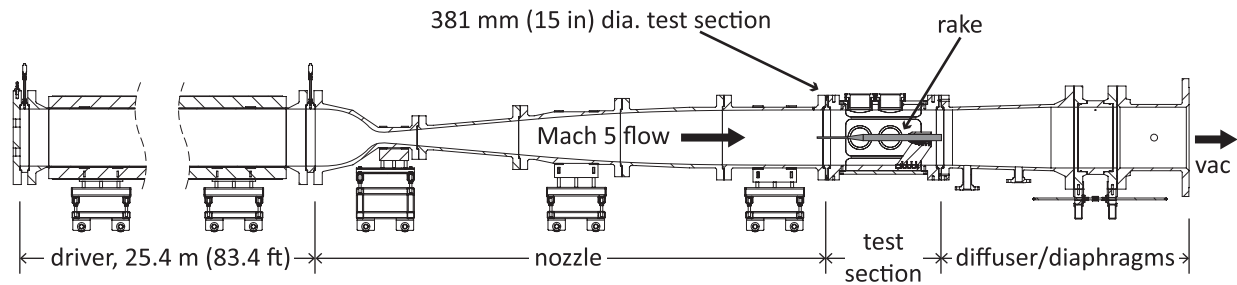
FIG. 1. Dimensioned schematic of LT5.

a 0.4 m (16 in.) inner diameter. The driver section is heated up to a maximum temperature of 453 K using blanket resistance heaters. Supply air is heated through convection with the hot surfaces as it enters the driver tube. This heating method is sufficient for the total temperature to reach equilibrium within 5–10 min of filling the tank depending on the fill pressure.

The 381 mm (15 in.) conventional nozzle was designed using the Sivells[8] method of characteristics (MoC) code coupled with the Harris and Blanchard[9] boundary layer solver. The contraction was designed using the matched cubic arc method of Morel.[10] The LT5 nozzle wall contour is depicted in Fig. 2 with the inviscid free-stream Mach number (M_∞) contour derived from the MoC solution. It features a slow expansion contour to approximate the length of a comparable quiet nozzle, resulting in a nozzle that is 3.5 m (11.5 ft) long. The tunnel has a quasi-steady run time of slightly longer than 100 ms.

The facility can operate at a range of total pressures and temperatures resulting in an estimated range of unit Reynolds number of $5.2 \times 10^6 \text{ m}^{-1} \leq Re' \leq 39.9 \times 10^6 \text{ m}^{-1}$, where the lower limit is an estimate and dependent on model blockage. Full tunnel operating parameters are summarized in Table I. The present flow characterization campaign focuses on the lower to middle portion of this operating range where free-stream noise levels are expected to be maximum.

LT5 operates using a downstream double diaphragm configuration. This approach results in a longer tunnel startup transient compared to an upstream diaphragm due to the need to pressurize the test section and is also more expensive per shot, but it prevents any debris from passing through the nozzle or test section and does not introduce any obstruction to the flow upstream of the nozzle like some fast-opening valves do. Both of these advantages are key considerations for its eventual quiet nozzle upgrade.[4] Multiple diaphragm materials have been tested for use in LT5, including Mylar®, 6061 Al, and 7075 Al with two scoring patterns for the latter two options. 6061 Al with a cross scoring pattern produced the most consistent burst pressure of the options tested and is now the standard diaphragm configuration.

The test section includes modular doors on all four sides, three of which typically feature optical access provided by sapphire windows (selected due to its high strength, hardness, and transmissivity
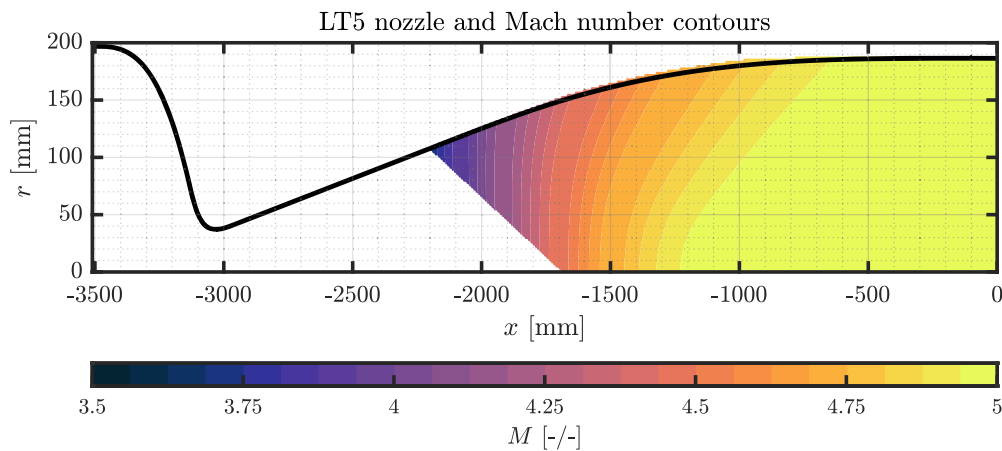

FIG. 2. Method of characteristics Mach number solution with the LT5 nozzle wall contour. Note: The horizontal axis is compressed compared to the vertical axis to enhance readability.

TABLE I. LT5 specifications and operating parameters. Minimum pressure (and dependent) values are approximate and vary with the installed model. Viscosity for Re' was calculated using Sutherland's law.

Parameter	Units	Range
Mach number, M_∞	–/–	4.84
Run time, t_{run}	ms	>100
Test-section diameter, D_{ts}	mm (in.)	381.0 (15.0)
Total pressure, p_{01}	kPa (psia)	344.7–2068.4 (50–300)
Total temperature, T_{01}	K (°F)	385–450 (233.3–350.3)
Unit Reynolds number, Re'	10^6 m^{-1} (10^6 ft^{-1})	5.2–39.9 (1.6–12.2)
Equivalent altitude	km (kft)	10.4–23.6 (34.1–77.4)
Dynamic pressure	kPa (psia)	12.9–77.4 (1.9–11.2)

of wavelengths ranging from ultraviolet through midwave infrared). The broadband optical transmissivity facilitates the use of infrared thermography using a FLIR X8500sc midwave infrared (MWIR) series camera while also allowing optical techniques utilizing wavelengths in the visible spectrum, such as schlieren. The windows have been treated with antireflective coatings to improve signal integrity for these optical measurements. The fourth modular door panel typically houses the model sting mount.

Air supplied to the driver tube is passed through two Parker DD60-08 300 psig desiccant air dryers and filtered with an IMI Norgren F46-800-AODA 250 psig filter to ensure only clean, dry air (CDA) is passed into the tunnel. A planned air infrastructure upgrade will soon allow CDA to be produced centrally rather than being filtered and dried at the point of use. Vacuum is generated for the facility by a Leybold SOGEVAC SV 630 B vacuum pump and a 20 m^3 (708 cu. ft) vacuum tank capable of maintaining a vacuum pressure of 0.1 torr. Prior to a run, the entire tunnel is evacuated (including the driver section) so that the system can be run entirely on CDA.

B. Instrumentation

Free-stream surveys were performed using a nine-probe Pitot rake depicted schematically in Fig. 3. Each transducer is mounted within a 4.7 mm (3/16 in.) diameter brass tube protruding 119.5 mm (4.7 in.) from the tip of the wedge base. The wedge mounts to a sting using one of several groups of mounting holes, allowing the probes to be repositioned in several spanwise (z) locations between runs in order to increase the spatial density and range of measurements. Incorporating all spanwise configurations, the rake can perform measurements across the test core and to within 7.6 mm (0.3 in.) of the tunnel walls. It can also be placed at streamwise locations ranging from 1000 mm (39.4 in.) upstream to 256.3 mm (10.1 in.) downstream of the nozzle exit. The probes are spaced $\Delta z = 40.6$ mm (1.6 in.) apart.

The measurement coordinate system is also shown in Fig. 3 where the y coordinate points out of the page and is aligned vertically with the lab reference frame. The origin of the coordinate system is placed at the center of the nozzle exit such that x is positive in the downstream direction. Note that only the x and z positions are varied in this campaign; the y coordinate is held constant at $y = 0$ at all measurement locations.

The rake was instrumented with Kulite XCE-062-20A pressure transducers fitted with A screens. The transducers were estimated to have a usable frequency bandwidth of 0–70 kHz based on the location of the resonance peak at ≈100 kHz. The signals were, therefore, low-pass filtered at 70 kHz to remove the cavity resonance and stopband from the data. Due to ongoing supply chain delays, only five transducers were available at the time of the first phase of this study in which streamwise profiles of noise and M_∞ were produced. The result is that only every other probe was instrumented with a transducer. Additional transducers were acquired and the port side probes were all filled for the second phase of the campaign involving the production of detailed spanwise profiles at several constant x locations.
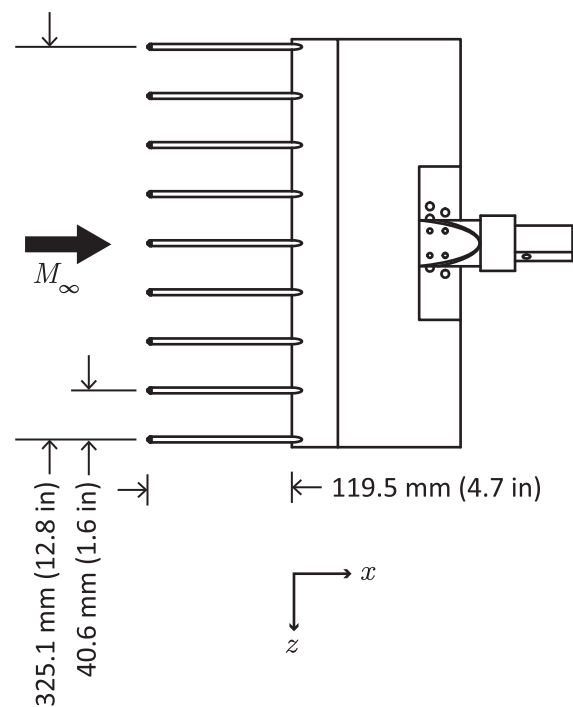

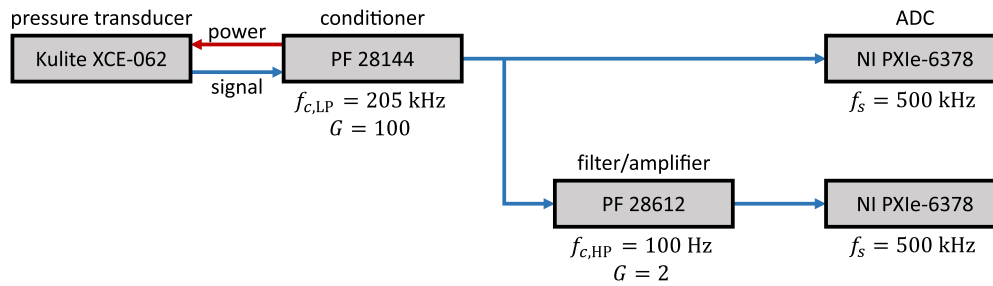**FIG. 3.** Dimensioned schematic of the Pitot rake with coordinate axes for reference.

FIG. 4. Process diagram depicting the signal conditioning and data acquisition systems used for the present experiments.

C. Data acquisition

Data were acquired using a National Instruments (NI) PXIe data acquisition system capable of sampling rates of up to 3.57 MS/s/ch with 16-bits of precision. Signal conditioning (excitation, amplification, and filtering) is provided by a Precision Filters (PF) 28 000 system. The facility currently offers up to 32 channels of transducer excitation and signal conditioning, 32 channels of 16-bit high-speed data acquisition, and 64 channels of thermocouples.

The PF conditioning system is built around a combination of model 28 144 transducer conditioner cards and model 28 612 filter/amplifier cards. The 28 144 cards provide transducer excitation, amplification ($G = 100$), and anti-aliasing filtration ($f_c = 205$ kHz). This signal is then split. One copy of the signal is sampled directly with a NI PXIe-6378 analog-to-digital converter ($f_s = 500$ kHz) to provide mean pressure data. The other copy is passed through a 28 612 card, where it is high-pass filtered ($f_c = 100$ Hz) and further amplified ($G = 2$) before being sampled to provide high-resolution fluctuating data. Figure 4 depicts a process diagram of the signal conditioning arrangement. After Pitot pressure data have been stored, they are digitally filtered to remove the spectral peaks due to cavity resonance.

Tunnel operating pressures—including total pressure in the reservoir (p_{01}), back pressure (p_b), and test-section pressure (p_1)—are measured with Omega pressure transducers and sampled at 5 kHz. The total temperature (T_0) is measured with a thermocouple located in the driver tube and sampled at 90 Hz.

III. RESULTS AND DISCUSSION

A. Mach number uniformity

The free-stream Mach number (M_∞) was measured at various x locations and multiple Re' conditions. Profiles generated by this set of measurements are depicted in Fig. 5. As part of the first phase of the experimental campaign, only five transducers were available, two of which were located inside the nozzle wall boundary layers and were, therefore, omitted from Mach number calculations. The availability of only three data points in the free stream at each streamwise location generally results in a relatively large uncertainty. Error bars were calculated using Student's t-distribution at the 95% confidence level.

As is evident in Fig. 5, M_∞ remains near 4.83 for all x and Re' values. While there do appear to be some undulations in M_∞, particularly at higher Re' values, most of the error bars overlap with
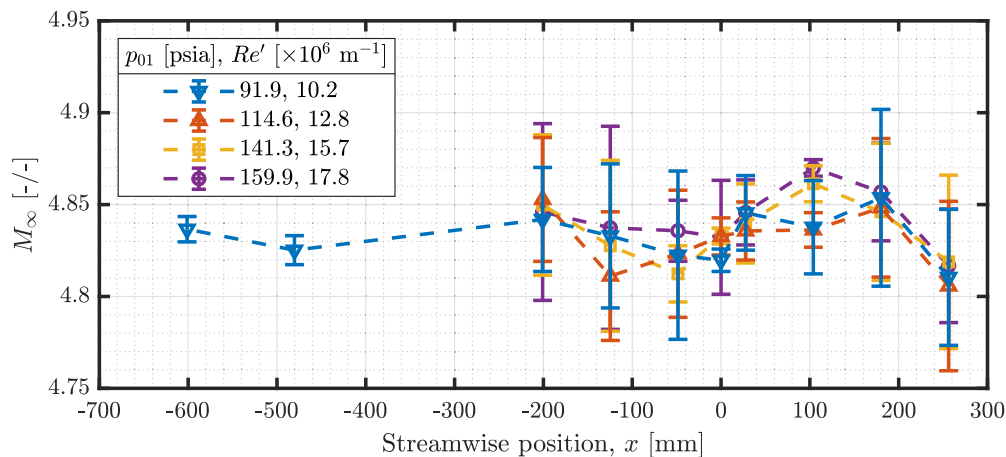

FIG. 5. Profiles of mean M_∞ vs x for various Re' conditions.

one another and a definitive conclusion can, therefore, not be drawn about this observation. The Mach number is lower than the design Mach number of 5 due to the fact that the nozzle was designed assuming a zero thickness boundary layer at the throat (i.e., assuming a leading edge exists near the throat such as due to a quiet nozzle bleed lip). In reality, the boundary layer has nonzero thickness entering the throat region, resulting in a thicker boundary layer and smaller effective expansion ratio compared to the design point.

In addition to the streamwise profiles of M_∞, several highly resolved spanwise profiles were measured at several locations along
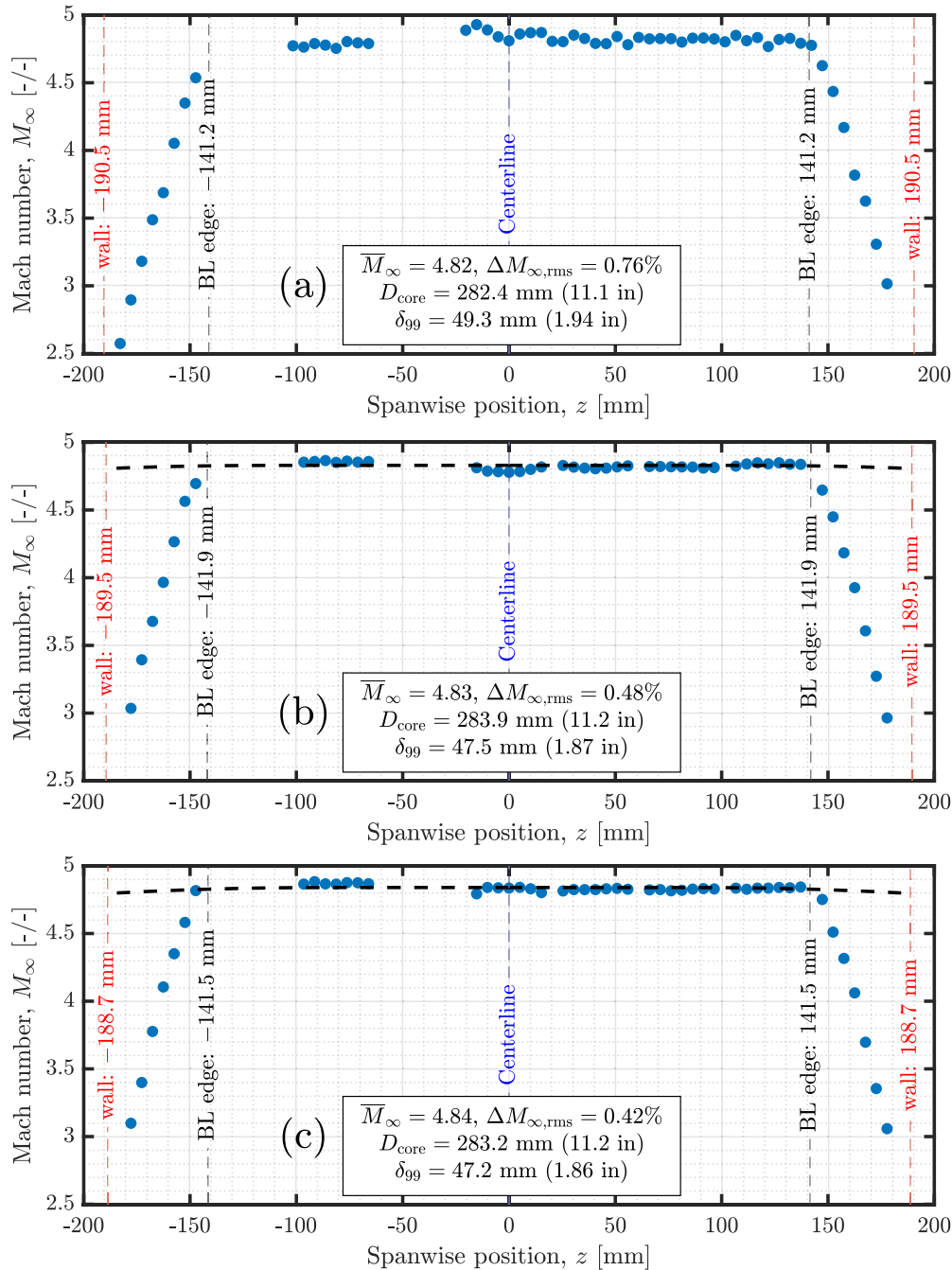

FIG. 6. High-resolution spanwise profiles of M_∞ vs z at $Re' = 10.1 \times 10^6$ m^{-1}. Scaled MoC solutions are provided for comparison at measurement stations located upstream of the nozzle exit. Profiles are shown at (a) $x = 0$ mm, (b) $x = -480$ mm, and (c) $x = -601$ mm.

the nozzle's length. These profiles were generated by adding two additional transducers to the port ($+z$) side of the rake and combining data from multiple runs at each location (eight at the exit and seven at other locations). For each run, the spanwise position of the rake was shifted by $\Delta z = 5.1$ mm (0.2 in.).

These profiles are depicted in Fig. 6 along with MoC solutions for comparison at the two upstream locations. The MoC solutions were rescaled by the mean measured M_∞ and used to compare the measured boundary layer thickness with the theoretical extent of the uniform inviscid flow region.

The spanwise M_∞ profile at the nozzle exit, $x = 0$ mm [Fig. 6(a)], shows excellent uniformity with the exception of a small peak at $z = -15$ mm and a smaller one at $z = 15$ mm. Mach lines traced upstream from this point do not intersect with any known feature of the nozzle contour (e.g., the seam between nozzle segments). Further, there is no periodicity in the profile matching the probe spacing, indicating that the peaks are not the result of bias introduced by run-to-run variability in flow conditions. Despite the peaks, the overall rms Mach number deviation across the inviscid core remains low at $\Delta M_{\infty,\mathrm{rms}} = 0.76\%$. The boundary layer thickness, calculated as the location where M is 99% of the free-stream value, was determined using a curve fit to the $+z$ data. At $x = 0$, $\delta_{99} \approx 49.3$ mm (1.94 in.) resulting in an inviscid core flow usable for testing with a diameter of 282.4 mm (11.1 in.).

Figures 6(b) and 6(c) depict the spanwise profiles of M_∞ at $x = -480$ and -601 mm, respectively. In each case, the peaks near the centerline are absent and the resulting rms Mach number deviations are considerably smaller at each location than at the exit: $\Delta M_{\infty,\mathrm{rms}}$ = 0.48% and 0.42%, respectively. All data points outside the boundary layer lie essentially on top of the MoC estimates depicted by the black dashed lines. There is no measurable change in Mach number across the span at any streamwise location, even when outside of the final expansion wave, due to the slow expansion contour design. The MoC solutions support this finding, as they do not appreciably change until well inside the boundary layer.

Finally, as the measurements move downstream, the boundary layer thickness increases slightly, resulting in a slightly smaller

inviscid core and slightly lower Mach number. The change represents less than a 0.5% reduction in M_∞ over the 600 mm measurement range and is, therefore, not expected to meaningfully affect future experimental results.

B. Free-stream acoustic noise

For each of the experimental results presented in Sec. III A, acoustic noise was also measured in the form of fluctuating Pitot pressure, $p'_{02,\mathrm{rms}}/\bar{p}_{02}$. Streamwise profiles of acoustic noise are presented in Fig. 7. There are two clear trends evident from the data: Acoustic noise increases as a function of x and decreases as a function of Re', both of which are consistent with prior observations by Pate and Schueler.[11] The mean acoustic noise level remains below 1.5% up to $z = 250$ mm and drops as low 1.0% in some regions at higher Re' conditions.

Figure 8 depicts spanwise profiles of acoustic noise at $x = 0$, -480, and -601 mm. Both the $x = 0$ mm case [Fig. 8(a)] and the $x = -601$ mm case [Fig. 8(c)] feature noise peaks located slightly outboard of the centerline. In each case, Mach lines traced upstream do not appear to intersect with any known feature or defect in the nozzle. It is plausible that manufacturing defects such as an imperceptible surface waviness could exist, resulting in a Mach wave focusing effect that results in higher noise near the centerline. This phenomenon has been previously described by Anders, Stainback, and Beckwith.[12]

At all locations, the noise level was increased somewhat near the centerline and minimal just outside of the boundary layer. At no point in any of the measurement regions does the noise level eclipse 1.6%, while at $x = -601$ mm, the local noise level drops below 1% near the boundary layer edge.

The power spectral density (PSD) of the acoustic noise at $x = 0$ mm was calculated using Welch's method.[13] The spectra, depicted at several z locations in Fig. 9, were bandpass filtered at 1 and 70 kHz to remove the DC signal and cavity resonance peak, respectively. At all z locations, the acoustic noise spectrum has two distinct regions in the passband which are approximately pink, i.e., $S_{pp} \propto 1/f^\alpha$. For
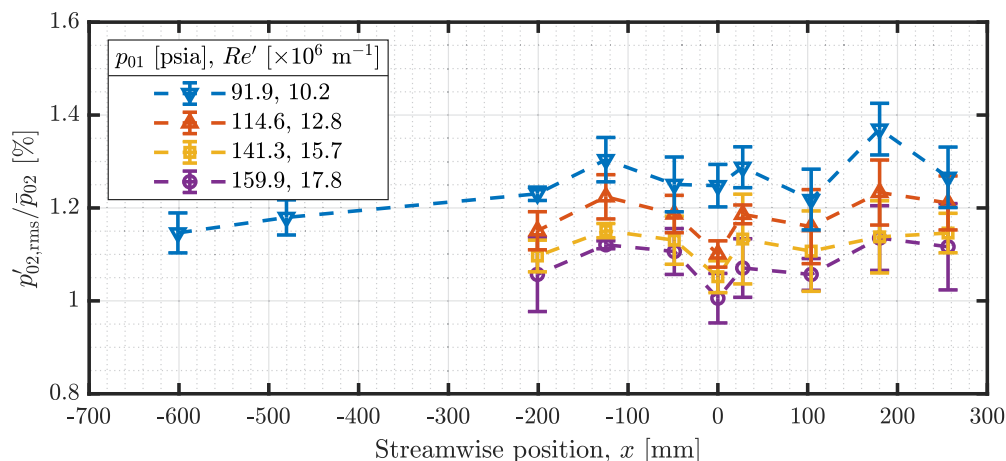

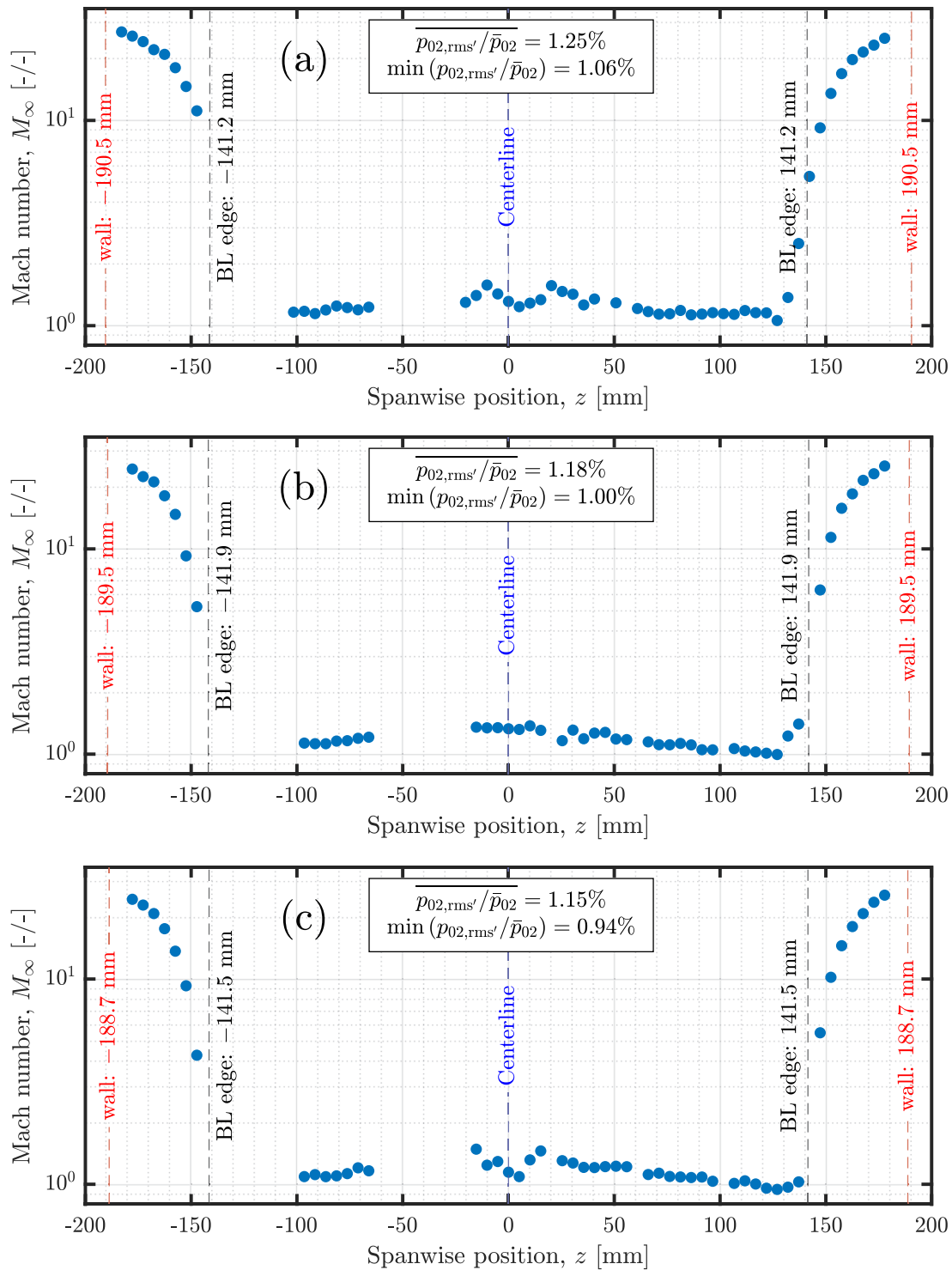**FIG. 7.** Profiles of mean free-stream acoustic noise vs x for various Re' conditions.

FIG. 8. High-resolution spanwise profiles of acoustic noise vs z at $Re' = 10.1 \times 10^6$ m^{-1}. Scaled MoC solutions are provided for comparison at measurement stations located upstream of the nozzle exit. Profiles are shown at (a) $x = 0$ mm, (b) $x = -480$ mm, and (c) $x = -601$ mm.
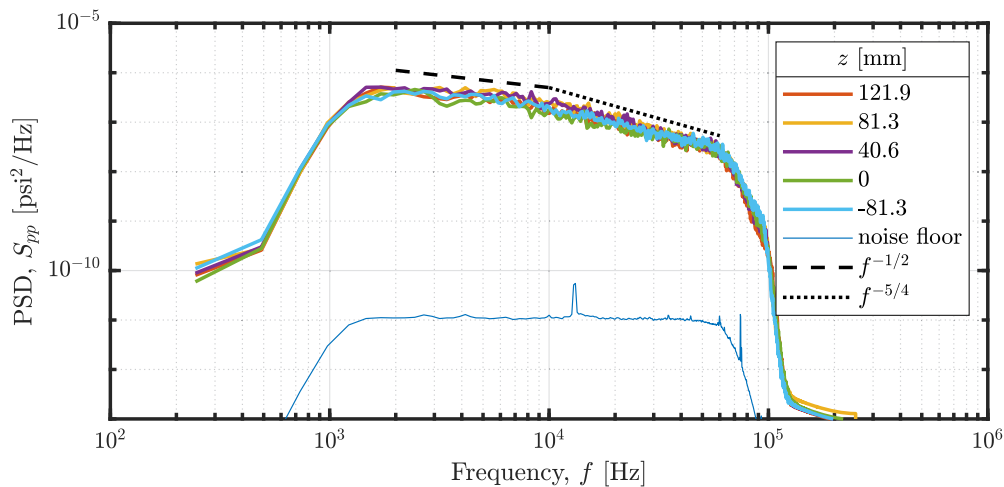
FIG. 9. Power spectral densities taken at the nozzle exit at various spanwise positions. Dashed lines highlight distinct regions with different slopes. $Re' = 10.1 \times 10^6$ m^{-1}.

$f < 10^4$ Hz, $\alpha \approx 1/2$, while for $f > 10^4$ Hz, $\alpha \approx 5/4$. Lines with these slopes are overlaid on Fig. 9. These values of α as well as the frequency at which the spectra transition from one region to the next are independent of z.

IV. CONCLUSION

A new Mach 5 Ludwieg Tube has been installed and calibrated at the UArizona. Its free-stream Mach number and acoustic noise level have been characterized by undertaking a series of measurement campaigns utilizing a Pitot rake outfitted with high-frequency pressure transducers. Overall flow uniformity was found to be good, with the maximum Mach number deviation of $\Delta M_{\infty,\mathrm{rms}}$ = 0.76% at the nozzle exit and $\Delta M_{\infty,\mathrm{rms}} < 0.50\%$ at all other measurement locations. Free-stream noise levels, characterized by measuring $p'_{02,\mathrm{rms}}/\bar{p}_{02}$, were generally low, with average noise levels across the span between 1.0% and 1.5% and local noise levels never exceeding 1.6% in the regions measured.

The spanwise noise profiles in some cases feature peaks located just outboard of the centerline. These peaks have no discernible cause and may be the result of machining defects creating Mach waves that are focused near the centerline. The appearance of peaks on both sides of the centerline suggests it is likely an axisymmetric surface waviness effect as opposed to a localized blemish. A similar peak in M_∞ was recorded at the nozzle exit, albeit only on one side of the centerline. Its cause is undetermined.

Spectra exhibit two regions of pink noise with a transition between the two that is independent of z. The reason for the change in slope is not yet known, nor is its dependence on Re'. Additionally, there may still be considerably fluctuating power at higher frequencies that were filtered when removing the resonant peak. Follow-up experiments are planned using dual Pitot probes with Kulite XCE-062 transducers adjacent to a higher-frequency transducer to extend the spectra over a wider bandwidth. Additionally, oversampling will improve frequency resolution to allow better exploration of lower frequencies and the transition between the two slopes in the spectra.

A quiet nozzle upgrade for LT5 is planned for a future date, which will undergo a similar characterization process. Additional transducers will be employed in order to reduce the uncertainty in each set of measurements. Hot-wire anemometry will also be explored as a tool for quantifying the vortical and temperature components of free-stream noise, an effort pioneered by Muñoz et al.[14]

AUTHOR DECLARATIONS

Conflict of Interest

The authors have no conflicts to disclose.

Author Contributions

Kyle P. Bearden: Formal analysis (lead); Investigation (lead); Methodology (equal); Writing – original draft (lead); Writing – review & editing (equal). **Victor E. Padilla:** Investigation (supporting). **Lutz Taubert:** Investigation (supporting); Methodology (equal). **Stuart A. Craig:** Conceptualization (lead); Formal analysis (supporting); Funding acquisition (lead); Supervision (lead); Writing – original draft (supporting); Writing – review & editing (lead).

DATA AVAILABILITY

The data that support the findings of this study are available from the corresponding author upon reasonable request.

REFERENCES

[1] H. Ludwieg, "Tube wind tunnel: A special type of blowdown tunnel," in *Eleventh Meeting of the Wind Tunnel and Model Testing Panel* (AGARD Rep. Scheveningen, Holland, 1957), Vol. 143.

[2] A. J. Cable and R. N. Cox, "The Ludwieg pressure-tube supersonic wind tunnel," Aeronaut. Q. **14**, 143–157 (1963).

[3] S. P. Wilkinson, S. G. Anders, and F.-J. Chen, "Supersonic and hypersonic quiet tunnel technology at NASA Langley," in AIAA 17th Aerospace Ground Testing Conference, Nashville, TN, 1992.

[4] S. P. Schneider, "Development of hypersonic quiet tunnels," J. Spacecr. Rockets **45**, 641–664 (2008).

[5] S. P. Schneider and C. E. Haven, "Quiet-flow Ludwieg tube for high-speed transition research," AIAA J. **33**, 688–693 (1995).

[6] T. J. Juliano, S. P. Schneider, S. Aradag, and D. Knight, "Quiet-flow Ludwieg tube for hypersonic transition research," AIAA J. **46**, 1757–1763 (2008).

[7] J. T. Flood, L. Taubert, and S. A. Craig, "Flow quality mapping of the Mach 4 quiet Ludwieg tube," in AIAA Scitech 2020 AIAA 2020-0360, 2020.

[8] J. C. Sivells, "A computer program for the aerodynamic design of axisymmetric and planar nozzles for supersonic and hypersonic wind tunnels," Tech. Rep. (AEDC-TR-78-63, 1978).

[9] J. E. Harris and D. K. Blanchard, "Computer program for solving laminar, transitional, or turbulent compressible boundary-layer equations for two-dimensional and axisymmetric flow," Tech. Rep. NASA TM-83207, 1982.

[10] T. Morel, "Comprehensive design of axisymmetric wind tunnel contractions," J. Fluids Eng. **97**, 225 (1975).

[11] S. R. Pate and C. J. Schueler, "Radiated aerodynamic noise effects on boundary layer transition in supersonic and hypersonic tunnels," AIAA J. **7**, 450–457 (1969).

[12] J. B. Anders, P. C. Stainback, and I. E. Beckwith, "New technique for reducing test section noise in supersonic wind tunnels," AIAA J. **18**, 5–6 (1980).

[13] P. Welch, "The use of fast Fourier transform for the estimation of power spectra: A method based on time averaging over short, modified periodograms," IEEE Trans. Audio Electroacoust. **15**, 70–73 (1967).

[14] F. Muñoz, J. Wu, R. Radespiel, M. Semper, R. Cummings, L. Duan, and T. Schilden, "Freestream disturbances characterization in Ludwieg tubes at Mach 6," in *AIAA Scitech 2019, January* (American Institute of Aeronautics and Astronautics, Reston, Virginia, 2019), pp. 1–21.